

Journal of Pakistan Institute of Chemical Engineers



journal homepage: www.piche.org.pk/journal

DOI: https://doi.org/10.54693/piche.5214



Effect of Grit Blasting on In-Vitro Bio-Assessment of Anodized and Electrodeposited HA-Coated AZ31B Magnesium Alloy

F. Hussain*1, M. U. Manzoor¹, M. Kamran¹, M. T. Z. Butt¹, T. Ahmad¹, F. Riaz¹
Submitted: 06/04/2024, Accepted: 21/06/2024, Online: 24/06/2024

Abstract

In this study, AZ31B Magnesium alloy samples were grit blasted with quartz and alumina particles at 1000 kPa blasting pressure to achieve sample roughness. The blasted samples were anodized and electrodeposited HA-coated for 40 minutes to improve the corrosion resistance and biocompatibility. The coating characteristics and composition of the coatings were studied by scanning electron microscopy (SEM) and energy dispersive X-ray (EDX) analysis respectively. The thickness of the coatings was measured using optical microscope. The corrosion behavior of the coatings was determined by open circuit potential (OCP) in a simulated body fluid (SBF) solution. The biocompatibility of the coatings was analyzed by bio-assessment using MTT assay. The results revealed that the electrodeposition of HA coating on alumina blasted samples results in best surface morphology, yielding lowest corrosion rate and best biocompatibility with a cell viability about 80% even after 7 days treatment.

Keyword: AZ31B magnesium alloy, Grit blasting, Blasting Pressure, Biocompatibility, Corrosion Resistance

1. Introduction:

Magnesium and its alloys are gaining significant interest in the field of metallic biomaterials due to their biodegradable nature, low density, exceptional biocompatibility, and particularly Young's modulus similar to that of natural bone which minimizes the stress shielding effect commonly observed in conventional metallic biomaterials like titanium alloys and stainless steels [1-5]. The biodegradable materials undergo degradation on interaction with a natural physiological environment and fully dissipate upon completion of their tissue regeneration supportive function, hence eliminating the need for post-surgery removal of the implant [6]. Magnesium,

which ranks as the fourth most common element present in the human body [7], produces harmless byproducts. Any excess magnesium will be eliminated through natural metabolic processes [8,9]. The relatively high degradation rate of magnesium severely limits its use in implant and tissue applications as the excessive release of hydrogen gas causes undesired interactions with tissues leading to the disruption of the healing process [10]. This phenomenon also results in the alkalization of the surrounding area of the wounded tissues leading to a reduction in the mechanical integrity of the implant-tissue interface [11,12].

Various methodologies have been investigated to minimize degradation rate including alloying,

¹Institute of Metallurgy & Materials Engineering, Faculty of Chemical & Materials Engineering, Quaid-e-Azam Campus, University of the Punjab, 54590. Lahore, Pakistan,

surface modification, and coatings [13,14]. The effect of milling variables, particularly ball size and milling time, on the mechanical properties and cytocompatibility of Mg-Zn-Co ternary alloy was investigated by Sehrish et al [15]. They reported that these variables have a significant influence on the mechanical characteristics and cytocompatibility of ternary alloy. Kumar et al. [16] studied the effect of alloying elements on the performance of a biodegradable magnesium alloy. The findings revealed that the degradation rate of the alloy can be effectively regulated by reducing the corrosion rate through appropriate alloying with elements such as Zr, Sr, Zn, Ca, Al, Mn, as well as rare earth elements resulting enhanced biocompatibility. Hussain et al. [17] examined the anodization of AZ31B magnesium alloy by two different electrolytes. The results revealed that anodic film provides better biodegradability. The effect of current density on the surface morphology, electrochemical behavior and biocompatibility of anodized AZ31B magnesium alloy was investigated by Oliveira et al [18]. The outcomes indicated that a denser anodic layer, superior corrosion resistance, and favorable biocompatibility were achieved at a 20 mA/cm² current density. Jamesh et al. [19] developed a HA coating on magnesium by electrodeposition and their research showed that this method is effective for developing Mg-based degradable implants and enhancing the corrosion resistance of CP-Mg in SBF. The influence of electrodeposition current density on the formation, coating characteristics and electrochemical behavior of HA coated AZ31B magnesium alloy was studied by Uddin et al [20]. The findings of their study indicated that a lower current density is more advantageous in the development of a corrosionresistant barrier layer for a biodegradable

magnesium implant. Pompa et al. [21] studied the corrosion resistance and biocompatibility of AZ31B, AZ91E and ZK60A magnesium alloys. According to their findings, anodized surfaces had a lower corrosion rate than untreated surfaces and, additionally, in vitro investigation showed that AZ91 and AZ31 alloys were cytocompatible with cell viability levels above 75%. The cytotoxicity response of three different cell lines with a magnesium alloy was examined by Mochizuki et al. [22] through direct cell cultivation on metal plates, as well as by assessing the cytotoxicity of individual metal ions. The findings indicated that a decrease in cell viability on the Mg samples in comparison to SUS316L and the cell morphologies observed on the surfaces exhibited irregular shapes, indicating cellular stress.

As discussed above there are several studies on the coating characteristics, corrosion behavior and cytocompatibility of anodized and electrodeposited HA-coated AZ31B magnesium alloy, however, the effect of surface roughness towards these coatings and their cytocompatibility has not been investigated. The current research work focused on the in-vitro bioassessment of anodized and electrodeposited HA-coated AZ31B magnesium alloy utilizing MC3T3 cell lines will provide insights into the influence of surface roughness on the biocompatibility and viability of the alloy.

2. Materials and Methods:

2.1 Sample Preparation:

Commercially available AZ31B Magnesium alloy sheet samples were grit blasted to obtain a rough surface. The selected grit blasting variables for the current study are listed in Table 1. After grit blasting, the surfaces were cleaned ultrasonically in an acetone bath for 30 minutes and dried for 15 minutes.

Table 1: Grit Blasting Variables

Abrasive Type	Abrasive Size (mesh)	Blasting Pressure (kPa)	Blasting Angle (degree)	Blasting Distance (mm)	Blasting Time (s)
Alumina	<200 μm	1000	90	10	20
Quartz	<200 μm	1000	90	10	20

2.2 Coatings Preparation & Characterization

Following the grit blasting process, anodized and HA-coated layers were developed on the grit blasted samples separately by anodization treatment and electrodeposition process respectively. The anodization treatment was carried out in an electrolyte having the composition listed in Table 2.

Table 2: Electrolyte for Anodization Treatment

Substance	Na ₃ PO ₄	КОН	KF	Al(NO 3)3	Na ₂ SiO ₃	Ethylene Glycol	Deionized Water
Amount	8.197 g	42.08 g	0.15 g	1.25 g	$0.075\mathrm{g}$	125 ml	125 ml

The grit blasted AZ31B magnesium alloy were used as the anode, while the graphite was used as the cathode. The samples were anodized at constant voltage of 20V for 40 minutes at room temperature.

Finally, the anodized samples were rinsed with deionized water and dried in warm air.

The HA coating was carried out in an electrolyte having the composition as listed in Table 3.

Table 3: Electrolyte for Hydroxyapatite Coating

Substance	Ca(NO ₃) ₂	NH ₄ H ₂ PO ₄	NaNO ₃	$\mathrm{H_{2}O_{2}}$	Deionized Water
Amount	2.8 g	1.16 g	3.4 g	8 ml	392 ml

The electrodeposition process was performed using a Potentiostat (Gamry Interface 1000E) with a three-electrode system at −1.4V applied potential for 40 minutes at room temperature. The samples were then immersed in 0.25 M NaOH solution for 2 hours at 60°C. As a result, the hydroxyapatite (HA)

coating was developed on the grit blasted sample. Afterwards, the samples were washed a few times in deionized water and air-dried for 2 to 3 hours.

The nomenclature of the samples to identify the process parameters is given in Table 4.

 Table 4: Nomenclature of Samples

Sample Labelling	Description		
PS	Pristine Sample		
Q1000-AT40	Quartz blasted sample, blasted at 1000 kPa blasting pressure and anodized for 40 minutes		
A1000-AT40	Alumina blasted sample, blasted at 1000 kPa blasting pressure and anodized for 40 minutes		
Q1000-HA40	Quartz blasted sample, blasted at 1000 kPa blasting pressure and HA-coated for 40 minutes		
A1000-HA40	Alumina blasted sample, blasted at 1000 kPa blasting pressure and HA-coated for 40 minutes		

The surface morphology of coatings was analyzed by scanning electron microscopy (SEM, FEI Inspect S50), and the elemental composition of the coating was determined using energy dispersive X-ray

analysis (EDX). The thickness of the coatings was measured with an optical microscope (Leica DMI5000 M).

2.3 Electrochemical Testing:

Potentiostat (Gamry Interface 1000E) was used to investigate the electrochemical behavior of coated samples using open circuit potential (OCP) in Ringer's lactate solution kept at 37°C for one hour. The electrochemical studies utilized a three-electrode system consisting of a graphite rod (counter electrode), Ag/AgCl saturated KCl (reference electrode) and coated sample (working electrodee). The exposed sample area was 1 cm².

2.4 Biocompatibility Analysis:

In vitro study, experiments are frequently conducted to assess the possible effects of the substance on the host cells before implantation. In most cases, international standards serve as the basis and description for such procedures. International standards like ISO-10993-5 and ISO-10993-12 are commonly used by researchers to evaluate different grades of magnesium [23-30]. Experimental assessments are recommended for biomaterial screening, with direct and indirect methods being indicated as potential approaches. An indirect approach has been adopted in this study. Magnesium materials were immersed in media for a specific duration to prepare the extracted solution samples. MTT assay was used to analyze the cytotoxicity potential of samples. This study aimed to examine the viability of cells using an extracted medium from the anodized and the HA-coated AZ31B Magnesium Alloy samples. The cell viability assays were conducted by monitoring the growth of MC3T3-E1 cells over 7 days.

The best anodized and electrodeposited HA-coated samples based on OCP measurement were subjected to biocompatibility analysis. The samples were sterilized for 2 hours under UV radiation and were immersed in serum-free Dulbecco's modified Eagle medium (DMEM) for 48 hours at 37°C with a surface area to extraction medium ratio of 1 cm²/ml to get the extract solution, which was stored at 4°C. The Mouse MC3T3-E1 cells, obtained from the American Type Culture Collection (ATCC), were cultivated in DMEM having 5% Penicillin/Streptomycin and 10% fetal bovine serum at 37°C under 5% CO2 atmosphere. The

MC3T3-E1 cells were cultured in 96-well plates at a density of 1 x 106 cells per ml. Each group was allocated six wells. The cells were incubated for a period of 24 hours to facilitate cell attachment. Following the incubation period of 24 hours, the culture media was replaced with extraction solutions of samples. Cytotoxicity assays were carried out after 1, 4, and 7 days of culture. Cell cultured with normal DMEM were used as a control for the MTT assay. For each well, 10 µl of MTT solution was added and left to incubate for 4 hours. Following the incubation period, 100 ul of dimethyl sulfoxide was added to each well to dissolve the MTT crystals, and the resulting solution was transferred to an ELISA reader plate. Subsequently, the ELISA plate reader was employed to detect the absorbance of each well at a specific wavelength of 490 nm. The morphology of cells was analyzed using an optical microscope. The percentage of cell viability was determined by using the subsequent formula:

$$Cell \ Viability \ (\%) = \frac{OD_{Sample}}{OD_{Control}} \ x \ 100$$

3. Results and Discussion:

3.1 Characterization of Coatings:

the

micrographs of electrodeposited HA-coated quartz and alumina blasted samples at 1000 kPa blasting pressure for 40 minutes processing time are shown in Fig. 2. It is evident from the Fig. 2. that the micrograph of quartz blasted samples show a complete coverage of the surface with visible cracks. On the contrary, the micrographs of alumina blasted samples reveal a few very fine surface cracks.

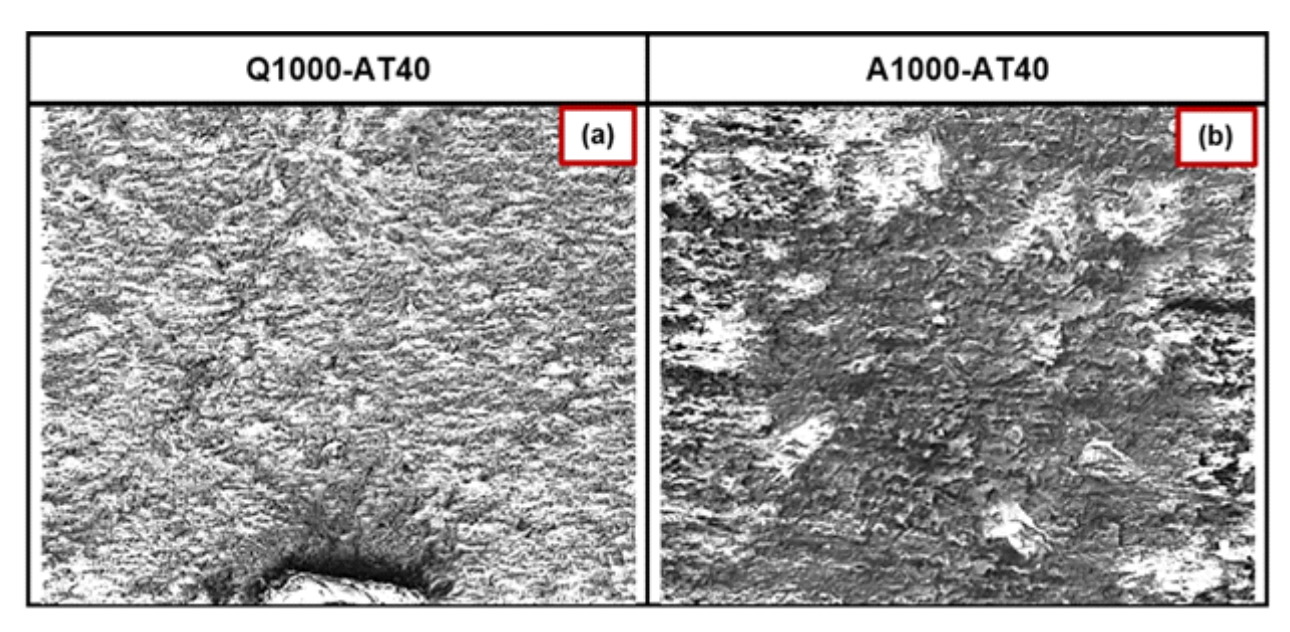


Figure 1. SEM micrograph of anodized samples (a) quartz blasted (b) alumina blasted

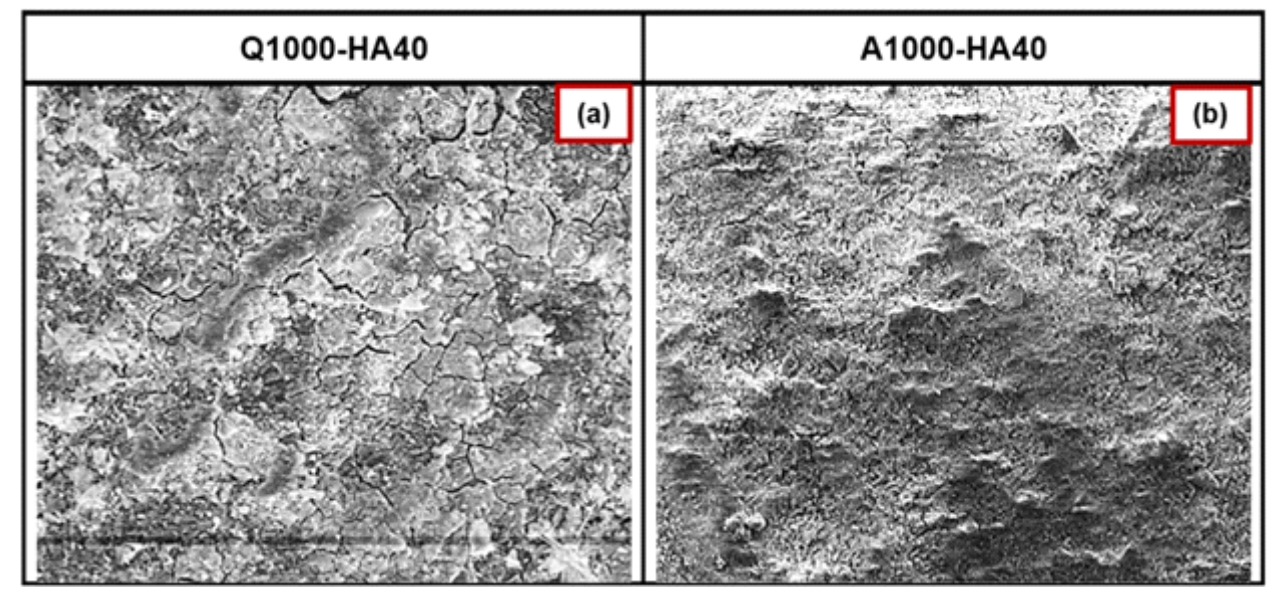


Figure 2. SEM micrograph of HA-coated samples (a) quartz blasted (b) alumina blasted

The coating thickness measurement from the cross-section of anodized and HA-coated samples, given in Table 4, clearly reveals that the average anodization coating and HA coating thicknesses of

alumina blasted samples are greater than that of quartz blasted samples with the similar blasting pressure and processing time.

Table 4. Average Coating Thickness Values

		s		
	Q1000-AT40	A1000-AT40	Q1000-HA40	A1000-HA40
Coating Thickness (µm)	2.01	2.03	11.72	11.83

The EDX analysis of anodized surface and hydroxyapatite deposited surface is shown in Figs. 3 and 4 respectively. The EDX analysis confirms the

presence of magnesium and oxygen elements in anodized coating and presence of calcium and phosphorous elements in HA coated samples.

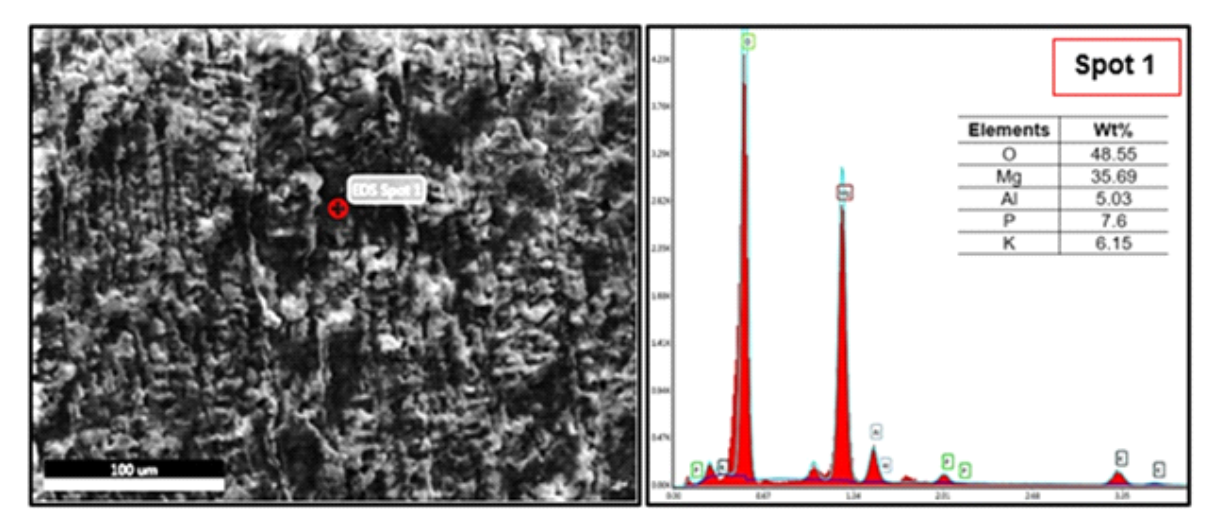


Figure 3. EDX analysis of anodized surface

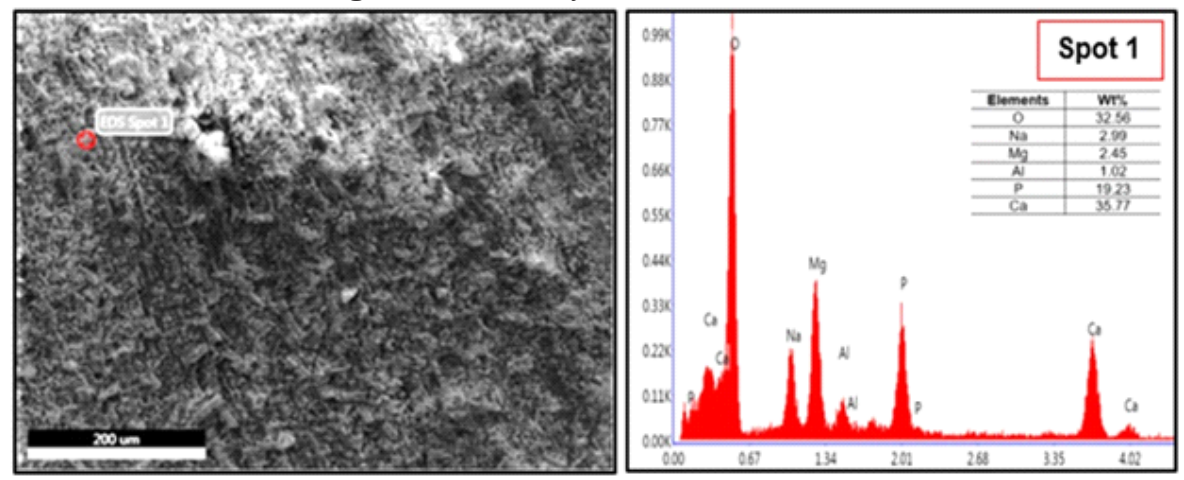


Figure 4. EDX analysis of hydroxyapatite deposited surface

3.2 Electrochemical Testing:

The open circuit potential refers to the thermodynamic tendency of a metal to undergo corrosion [31]. A low OCP signifies a strong thermodynamic tendency towards rusting. A higher OCP may suggest a state of passivation or a reduced

tendency for electron loss [32]. The OCP values of the anodized coating and HA coating of the samples under study are given in Table 5. The lower OCP values of anodized and HA-coated alumina blasted samples confirm the more compact and pore-free coatings than that of quartz blasted samples.

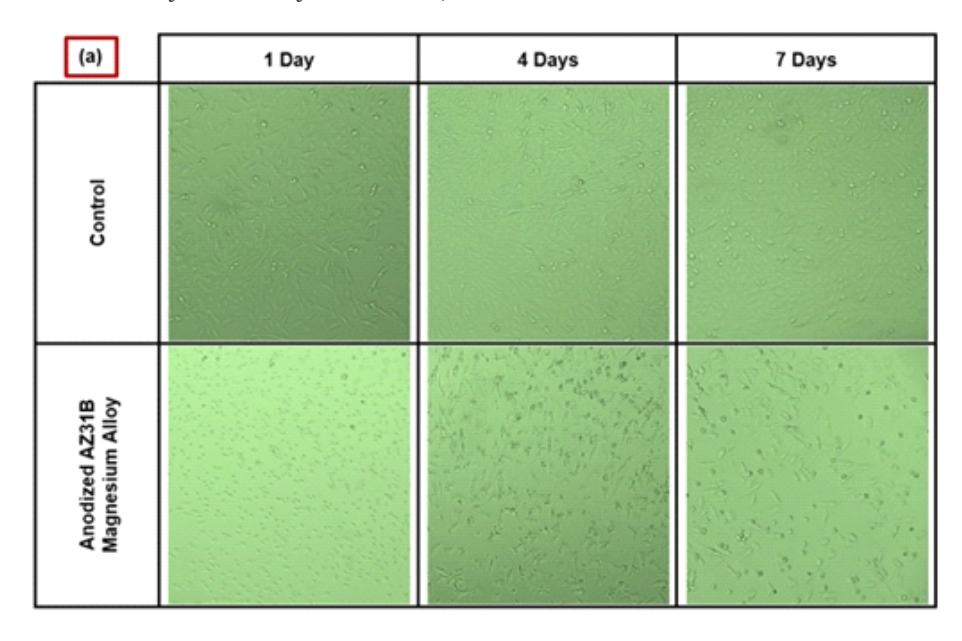
Table 5. Open Circuit Potential Values

		s		
	Q1000-AT40	A1000-AT40	Q1000-HA40	A1000-HA40
OCP (V)	-0.114	-0.065	-0.085	-0.049

3.3 Biocompatibility Analysis:

The optical images of the MC3T3-E1 cells grown in extract media are shown in Fig. 5(a). A correlation exists between net cell growth and cell viability data. The results showed that the extracted media from the anodized AZ31B magnesium alloy sample has good cell morphology. The outcomes of MTT assays of anodized samples are depicted in Fig. 5(b). The cells remained viable until day 1 and the rate of cell proliferation exceeded the 70%. Till the fourth day, the treatment had enhanced the viability of the cells, resulting in a proliferation rate of over 75%. Following an additional 3 days i.e. 7-day treatment,

it was observed that the overall cell count has increased and the cell proliferation rate being recorded was greater than 75%. The data demonstrated that the extracted media from the anodized AZ31B magnesium alloy sample had no negative influence on the viability and proliferation of the cells. Thus, it can be concluded that the cells cultivated with the incubated media exhibited significantly higher viability compared to the control viability i.e. 70%, confirming the compact and pore-free nontoxic anodized coating produced on alumina blasted samples of AZ31B magnesium alloy.



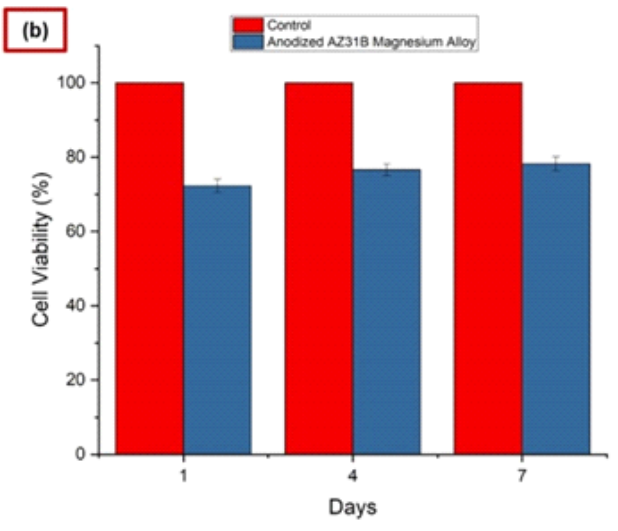
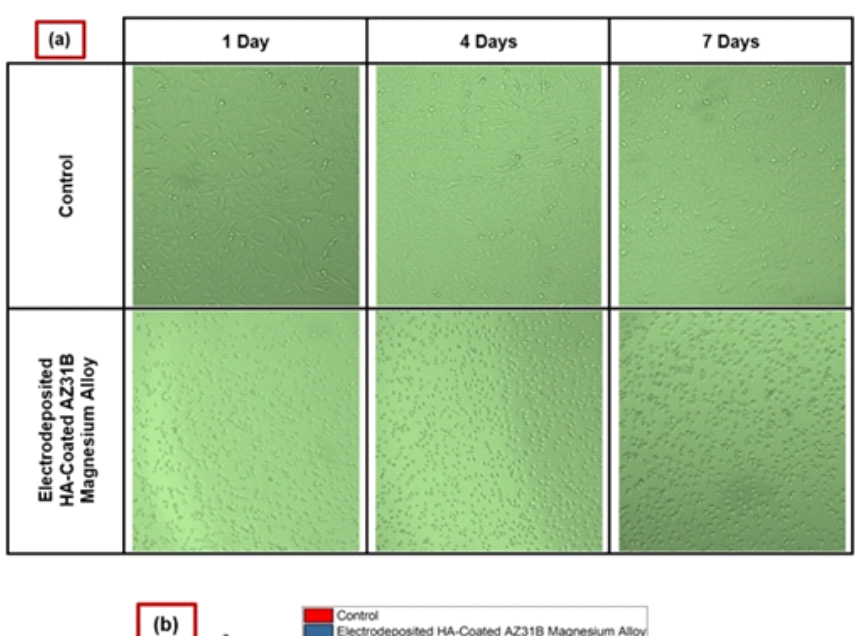


Figure 5. In-Vitro Biocompatibility Study of Anodized AZ31B Magnesium Alloy; (a) Microscopical Analysis of MC3T3-E1 Cells Cultured in Extracted Media (b) Viability of MC3T3-E1 Cells Cultured in Extracted Media

The optical images of the MC3T3-E1 cells grown in extract media are shown in Fig. 6(a). A correlation exists between net cell growth and cell viability data. The results showed that the extracted media from the electrodeposited HA-coated AZ31B magnesium alloy sample has best cell morphology. The findings of MTT assays of electrodeposited HA-coated samples are depicted in Fig. 6(b). The cells remained viable until day 1 and the rate of cell proliferation exceeded the 75%. Till the fourth day, the treatment had enhanced the viability of the cells, resulting in a proliferation rate of over 80%. Following an additional 3 days i.e. 7-day treatment,

it was observed that the overall cell count has increased and the cell proliferation rate being recorded was greater than 80%. The data demonstrated that the extracted media from the electrodeposited HA-coated AZ31B magnesium alloy sample had no negative influence on the viability and proliferation of the cells. Thus, it can be concluded that the cells cultivated with the incubated media exhibited significantly higher viability compared to the control viability i.e. 70%, confirming the compact and pore-free nontoxic HA-coating produced on alumina blasted samples of AZ31B magnesium alloy.



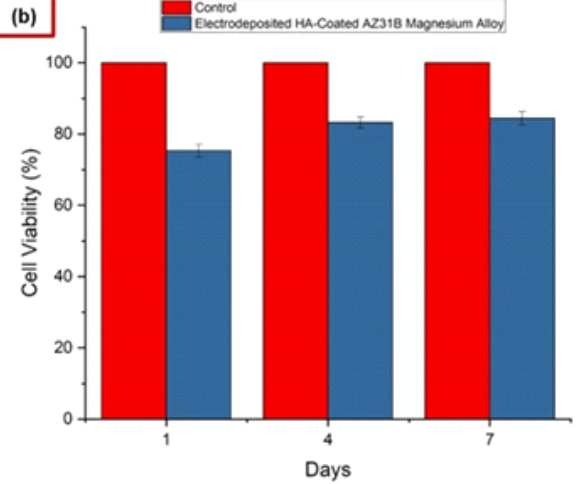


Figure 6. In-Vitro Biocompatibility Study of Electrodeposited HA-Coated AZ31B Magnesium Alloy; (a) Microscopical Analysis of MC3T3-E1 Cells Cultured in Extracted Media (b) Viability of MC3T3-E1 Cells Cultured in Extracted Media

4. Conclusions:

AZ31B magnesium alloy sheet samples were grit blasted with quartz and alumina particles at 1000 kPa blasting pressure. The grit blasted samples were anodized and electrodeposited with HA coating for processing time of 40 minutes. The coating layers were investigated to study the effect of surface roughness towards coatings and their cytocompatibility. Based on the experimental outcomes, it was concluded that:

A thicker anodized and electrodeposited HAcoating with full surface coverage were achieved on alumina blasted samples as compared to quartz blasted samples.

The electrochemical experiments demonstrated that the OCP values were better for alumina blasted samples particularly for HA-coated sample than that of quartz blasted samples.

The biocompatibility analysis displayed highest cell viability of electrodeposited HA-coated layer as compared to anodized layer developed on alumina blasted samples.

References:

- D. Zhao et al., "Current status on clinical applications of magnesium-based orthopaedic implants: A review from clinical translational perspective," Biomaterials, vol. 112, pp. 287–302, Jan. 2017.
- S. Julmi *et al.*, "Processing and coating of openpored absorbable magnesium-based bone implants," Mater. Sci. Eng. C, vol. 98, pp. 1073–1086, May 2019.
- 3. J. D. Barajas *et al.*, "Relationship between microstructure and formation-biodegradation mechanism of fluoride conversion coatings synthesised on the AZ31 magnesium alloy," Surf. Coatings Technol., vol. 374, pp. 424–436, Sep. 2019.
- 4. D. Lu *et al.*, "An approach to fabricating protective coatings on a magnesium alloy utilising alumina," Surf. Coatings Technol., vol. 367, pp. 336–340, Jun. 2019.
- 5. S. N. Dezfuli et al., "Advanced bredigite-

- containing magnesium-matrix composites for biodegradable bone implant applications," Mater. Sci. Eng. C, vol. 79, pp. 647–660, Oct. 2017.
- 6 M. Yazdimamaghani *et al.*, "Porous magnesium-based scaffolds for tissue engineering," Mater. Sci. Eng. C, vol. 71, pp. 1253–1266, Feb. 2017.
- 7. G. Zhang *et al.*, "In-situ grown super- or hydrophobic Mg-Al layered double hydroxides films on the anodized magnesium alloy to improve corrosion properties," Surf. Coatings Technol., vol. 366, pp. 238–247, May 2019.
- 8. Y. Guo *et al.*, "Effect of implantation of biodegradable magnesium alloy on BMP-2 expression in bone of ovariectomized osteoporosis rats," Mater. Sci. Eng. C, vol. 33, no 7, pp. 4470–4474, Oct. 2013.
- S. Fintová et al., "Degradation of unconventional fluoride conversion coating on AZ61 magnesium alloy in SBF solution," Surf. Coatings Technol., vol. 380, p. 125012, Dec. 2019.
- 10. A. Kopp *et al.*, "Influence of design and postprocessing parameters on the degradation behavior and mechanical properties of additively manufactured magnesium scaffolds," Acta Biomater., vol. 98, pp. 23-35, Oct. 2019.
- 11. M. Muñoz *et al.*, "PLA deposition on surface treated magnesium alloy: Adhesion, toughness and corrosion behaviour," Surf. Coatings Technol., vol. 388, p. 125593, Apr. 2020.
- 12. S. Jiang *et al.*, "Synthesis and characterization of magnesium phytic acid/apatite composite coating on AZ31 Mg alloy by microwave assisted treatment," Mater. Sci. Eng. C, vol. 91, pp. 218–227, Oct. 2018.
- 13. K. Catt *et al.*, "Poly (3,4-ethylenedioxythioph ene) graphene oxide composite coatings for controlling magnesium implant corrosion," Acta Biomater., vol. 48, pp. 530–540, Jan. 2017.
- 14. J. de O. Braga *et al.*, "Fabrication and characterization of dicalcium phosphate

- coatings deposited on magnesium substrates by a chemical conversion route," Surf. Coatings Technol., vol. 386, p. 125505, Mar. 2020.
- 15. S. Mukhtar *et al.* "A. Effect of Milling Parameters on Mechanical Properties and In Vitro Biocompatibility of Mg-Zn-Co Ternary Alloy", Metals, vol. 12, p. 529 Mar. 2022.
- 16. R. Kumar *et al.*, "Effects of alloying elements on performance of biodegradable magnesium alloy", Materials Today: Proceedings, vol. 56, pp. 2443-2450, Apr. 2022.
- 17. F. Hussain *et al.* "Surface Modification of AZ31B Magnesium Alloy by Anodization Process", Journal of Pakistan Institute of Chemical Engineers, vol. pp. 11-20, Mar. 2021.
- L. A. de Oliveira et al., "Surface chemistry, film morphology, local electrochemical behavior and cytotoxic response of anodized AZ31B magnesium alloy", Journal of Materials Research and Technology, vol. 9, pp. 14754-14770, Dec. 2020.
- M. Jamesh et al., "Electrodeposition of hydroxyapatite coating on magnesium for biomedical applications". J Coat Technol Res, vol. 9, pp. 495–502, Jul. 2012.
- 20 M. Uddin et al., "Fabrication, characterisation and corrosion of HA coated AZ31B Mg implant material: Effect of electrodeposition current density", Surface and Coatings Technology, vol. 385, p. 125363, Mar. 2020.
- 21. L. Pompa *et al.*, "Surface characterization and cytotoxicity response of biodegradable magnesium alloys", Mater Sci Eng C Mater Biol Appl., vol. 49, pp. 761-768, Apr. 2015.
- 22. A. Mochizuki *et al.*, "Cytocompatibility of magnesium and AZ31 alloy with three types of cell lines using a direct in vitro method.", J Mater Sci: Mater Med, vol. 27, Aug. 2016.
- 23. J. Fischer *et al.*, "Improved cytotoxicity testing of magnesium materials", Mater Sci Eng B, vol. 176, pp. 830–834, Jun 2011.
- 24. Y. Sun *et al.*, "In-vitro evaluation of Mg-4.0Zn-0.2Ca alloy for biomedical application", Trans. Nonferrous Met. Soc. China, vol. 21, pp. s252-s257, Aug. 2011.

- 25. J. Niu *et al.*, "Enhanced biocorrosion resistance and biocompatibility of degradable Mg–Nd–Zn–Zr alloy by brushite coating", Mater. Sci. Eng. C, vol. 33, pp. 4833–4841, Dec. 2013.
- 26. X. Gu *et al.*, "In vitro corrosion and biocompatibility of binary magnesium alloys", Biomaterials, vol. 30, pp. 484–498, Feb. 2009.
- 27. P. Gill *et al.*, "Corrosion and biocompatibility assessment of magnesium alloys", J. Biomater. Nanobiotechnol., vol. 3, pp. 10-13, Jan. 2012.
- 28. Z.G. Huan *et al.*, "In vitro degradation behavior and cytocompatibility of Mg–Zn–Zr alloys, J. Mater. Sci. Mater.Med., vol. 21, pp. 2623–2635, Jun. 2010.
- 29. D. Hong *et al.*, "In vitro degradation and cytotoxicity response of Mg-4% Zn-0.5% Zr (ZK40) alloy as a potential biodegradable material", Acta Biomater, vol. 9, pp. 8534-8547, Nov 2013.
- 30. S. Guan *et al.*, "Mg Alloys Development and Surface Modification for Biomedical Application", Magnesium Alloys Corrosion and Surface Treatments, 2011.
- 31. D. Wang *et al.*, "Sulfate Reducing Bacterium Desulfovibrio vulgaris Caused Severe Microbiologically Influenced Corrosion of Zinc and Galvanized Steel". Int. Biodeterior. Biodegrad., vol. 157, p. 105160, Feb. 2021.
- 32. T. Unsal *et al.*, "Assessment of 2,2-Dibromo-3-Nitrilopropionamide Biocide Enhanced by D-Tyrosine against Zinc Corrosion by a Sulfate Reducing Bacterium", Ind. Eng. Chem. Res., vol. 60, pp. 4009–4018, Mar. 2021.